JOURNAL OF BACTERIOLOGY, Feb. 1996, p. 977–984 Vol. 178, No. 4
0021-9193/96/$04.00+0

Suppression of a Signaling Defect during *Myxococcus xanthus* Development

KEESOO LEE† AND LAWRENCE J. SHIMKETS*

Department of Microbiology, University of Georgia, Athens, Georgia 30602

Received 25 September 1995/Accepted 30 November 1995

The *csgA* gene encodes an extracellular protein that is essential for cell-cell communication (C-signaling) during fruiting body development of *Myxococcus xanthus*. Two transposon insertions in the *socABC* operon, *soc-560* and *socC559*, restore development to *csgA* null mutants. Mixing *soc-560 csgA* cells or *socC559 csgA* cells with *csgA* cells at a ratio of 1:1 stimulated the development of *csgA* cells, suggesting that *soc* mutations allow cells to produce the C-signal or a similar molecule via a *csgA*-independent mechanism. The *socABC* operon contains the following three genes: *socA*, a member of the short-chain alcohol dehydrogenase gene family; *socB*, a gene encoding a putative membrane anchoring protein; and *socC*, a negative autoregulator of *socABC* operon expression. Both suppressor mutations inactivate *socC*, leading to a 30- to 100-fold increase in *socA* transcription; *socA* expression in suppressor strains is at least 100-fold higher than *csgA* expression during all stages of development. The amino acid sequence of SocA has 28% identity and 51% similarity with that of CsgA. We suggest that CsgA suppression is due to overproduction of SocA, which can substitute for CsgA. These results raise the possibility that a cell surface dehydrogenase plays a role in C-signaling.

Myxococcus xanthus cells subjected to nutritional stress initiate an ordered series of behavioral changes to produce a fruiting body containing dormant spores (for reviews, see references 13 and 54). Initially, cells accumulate in ridges that move processively to generate the appearance of traveling waves, which are referred to as ripples (57). Rippling is not absolutely required for later developmental events but is physiologically linked with fruiting body development in that it is also dependent on a cell-cell signaling gene known as *csgA*. Shortly after rippling is observed, cells begin gliding to aggregation centers at which they form a fruiting body. Development concludes with the differentiation of dormant myxospores within the fruiting body.

The efforts of large numbers of developing cells are channeled to common goals through the use of extracellular cell-cell signals that synchronize cell behavior and induce developmental gene expression. A major thrust in developmental biology is the identification of signaling molecules and elucidation of the perception and signal transduction pathways. Cell-cell interactions play an essential role in both morphological development and the expression of the stage-specific genes that compose the myxobacterial developmental program. The fruiting body development of *M. xanthus* is regulated by at least five different signals (A, B, C, D, and E), and the elimination of any of these signals by mutation disrupts development (11, 20). One of these, the C-signal, appears to act as a developmental timer which triggers each of the developmental behaviors, rippling, fruiting body formation, and sporulation at different extracellular concentrations (32, 41).

Each of the 10 known mutations that disrupt C-signaling maps to the *csgA* gene, which becomes transcriptionally active several hours after the initiation of development (21, 55, 56). *csgA* mutants become defective in the activation of developmental gene expression shortly thereafter (36, 42). Several lines of evidence suggest that CsgA is associated with the cell surface. First, *csgA* mutants can be stimulated to develop by direct contact with wild-type cells and extracellular complementation does not occur when wild-type and *csgA* mutant cells are separated by a membrane with a pore size of 0.45 μm (29). Second, CsgA purified from wild-type cells restores fruiting body formation and sporulation to *csgA* mutants (28, 29). Finally, anti-CsgA antibodies inhibit both fruiting body morphogenesis and sporulation of wild-type cells and decorate the cell surface and extracellular matrix (58). Cell motility is necessary to achieve optimal cell alignment for the presentation of CsgA to adjacent cells (30, 31).

The simplest conclusion from the observations described above is that CsgA is the C-signal (29). Recently, however, a class of second-site suppressors that restore *csgA* development has led to an alternative hypothesis that CsgA manufactures the C-signal through an enzymatic activity. Two transposon insertions, *socC559* and *soc-560*, efficiently restored rippling, aggregation, and sporulation to *csgA* null mutants (50). These mutations are located in the *socABC* operon, which contains the following three genes: *socA*, a member of the short-chain alcohol dehydrogenase (SCAD) family, like *csgA*; *socB*, a membrane anchoring protein; and *socC*, a gene with no homologous members in the database (formerly *socA1*, *socA2*, and *socA3*, respectively [39]). Both suppressor mutations are Tn*5 lac* insertions that are similarly oriented but located in different protein coding regions (Fig. 1). Tn*5 lac*ΩLS560 (*soc-560*) is located between *socA* and *socB*, and Tn*5 lac*ΩLS559 (*socC559*) is located in the 5′ end of *socC*. How do null mutations in the *socABC* operon restore a developmental pathway disrupted by a null mutation in *csgA*? We propose that *soc* mutations do so by derepressing the production of SocA, which has overlapping substrate specificity with CsgA and can manufacture the C-signal via a CsgA-independent pathway.

MATERIALS AND METHODS

Bacterial strains and growth conditions. The *M. xanthus* strains used are listed in Table 1. Vegetative cultures were grown at 32°C in CTT broth and plated on CTT agar (24). Liquid cultures were incubated in a New Brunswick G24 envi-

* Corresponding author. Mailing address: Department of Microbiology, University of Georgia, Athens, GA 30602. Phone: (706) 542-2681. Fax: (706) 542-2674. Electronic mail address: shimkets@bscr.uga.edu.

† Present address: Department of Anesthesiology, Duke University Medical School, Durham, NC 27710.

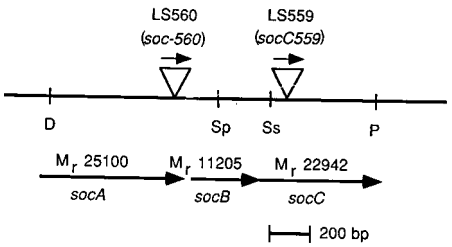

FIG. 1. The *socABC* operon. Triangles indicate the positions of the Tn*5 lac* insertions, with small arrows above them indicating the direction of *lacZ* transcription. Restriction enzymes: D, *Dra*I; Sp, *Sph*I; Ss, *Ssp*I; P, *Ppu*MI. Large arrows indicate polypeptide coding sequences, with the sizes of the putative products shown above the arrows and the gene names listed below. Bar, 200 bp of wild-type DNA sequence.

ronmental shaker at 325 rpm to enhance dispersed growth. Cells were harvested in the mid-exponential phase of growth (3×10^8 to 5×10^8 cells ml^{-1}). *Escherichia coli* was grown in L broth or on L agar.

DNA analyses. Deletion mutations were constructed by PCR-based unique-site elimination (8) using the Transformer site-directed mutagenesis kit (Clontech, Inc.). Several clones were analyzed by restriction digestion and DNA sequencing to confirm mutations. The P1 and P2 promoter deletion constructs were introduced into plasmid pLEE6 (39), which contains vector sequences that allow integration into the chromosome at the phage Mx8 attachment site *attB* (55).

The deletion of the entire *socABC* operon was accomplished by replacing the sequences between the unique *Dra*I and *Ppu*MI restriction sites (Fig. 1) with a unique *Ssp*I site into which the kanamycin resistance gene from Tn5 (27) was inserted. A plasmid containing this construct, pLEE19, was transduced into *M. xanthus* LS523 (*csgA205*) by bacteriophage P1-mediated transduction (56). This plasmid cannot replicate but does undergo homologous recombination at the *socABC* operon by either single crossover or double crossover. Double crossover leads to replacement of the native operon with the deleted operon and elimination of the vector sequences. Kanamycin-resistant transductants were screened by colony hybridization with a vector-specific probe, pUC19, to determine which type of crossover event occurred. Each of 430 transductants was derived from a single crossover.

The disruption of *socA* was also attempted by homologous integration of a truncated *socA* gene lacking essential 5′ and 3′ sequences. A 0.45-kbp *Eag*I-*Eag*I internal fragment of *socA* was inserted into pBR322 to create pLEE52. The *Eag*I-*Eag*I fragment lacks 54 codons from the 5′ of *socA* and 45 codons from the 3′ end. The integration of this plasmid into *socA* by homologous recombination results in two incomplete copies of *socA* separated by vector sequences (55). No viable transformants were detected.

TABLE 1. Myxobacterial strains

Strain	Genotype[a]	Reference or derivation
DK1622	Wild type	57
LS204	*csgA731*	55
LS205	*csgA205*	55
LS293	*socC-lacZ*/*socC*$^+$	39
LS295	*csgA205 socC-lacZ*/*socC*$^+$	P1(pLEE1[b]) × LS523
LS523	*csgA205*	55
LS559	*csgA205 socC559*	50
LS560	*csgA205 soc-560*	50
LS620	*socC559*	39
LS641	*socC-lacZ*/*socC*$^+$	P1(pLEE6[c]) × DK1622
LS642	Δ*P1socC-lacZ*/*socC*$^+$	P1(pLEE43[d]) × DK1622
LS643	Δ*P2socC-lacZ*/*socC*$^+$	P1(pLEE44[d]) × DK1622
LS644	*socC-lacZ*/*socC*$^+$ *csgA205*	P1(pLEE6[c]) × LS523
LS645	Δ*P1socC-lacZ*/*socC*$^+$ *csgA205*	P1(pLEE43[d]) × LS523
LS646	Δ*P2socC-lacZ*/*socC*$^+$ *csgA205*	P1(pLEE44[d]) × LS523

[a] A shill indicates that the strain is a merodiploid for the alleles given.
[b] Plasmid pLEE1 contains a *socC-lacZ* transcriptional fusion that is integrated by homologous recombination at the *socABC* operon (39).
[c] Plasmid pLEE6 contains a *socC-lacZ* transcriptional fusion that is integrated at the Mx8 *attB* site (39).
[d] Plasmids pLEE43 and pLEE44 are identical to pLEE6, except for 20-bp deletions in the *socABC* operon upstream region (Fig. 7).

DNA and amino acid sequences were analyzed with the University of Wisconsin Genetics Computer Group software package (9).

RNA purification and analysis. RNA was extracted from vegetative cells with urea buffer (8.0 M urea, 350 mM NaCl, 50 mM Tris-HCl [pH 7.5], 20 mM Na_2EDTA, 2% [wt/vol] Sarkosyl, 5% [vol/vol] phenol) and purified as previously described (21), with modifications. After the two LiCl precipitation steps, RNA was ethanol precipitated and then incubated at 37°C for 30 min with RNase-free DNase (Promega). The analysis of RNA by slot hybridization was similar to that previously described (62), with modifications. Each RNA sample was diluted 10-fold with a denaturing solution containing 50% formamide, 6% formaldehyde, and 10 mM $NaH_2PO_4 \cdot Na_2HPO_4$ buffer (13.8 mg of monosodium–241 mg of disodium phosphate in 100 ml), heated for 15 min at 65°C, chilled on ice, and mixed with an equal volume of 20× SSC (1× SSC is 0.15 M NaCl plus 0.015 M sodium citrate). A volume of 200 μl containing 2 μg of RNA was added to each slot with a minifold apparatus (Schleicher and Schuell, Inc., Keene, N.H.), and the filter was baked for 2 h at 80°C. A 1-kbp *Dra*I-*Sph*I restriction fragment containing most of the *socA* gene and a portion of *socB* (Fig. 1) was labeled with [α-^{32}P]dCTP to a specific activity of about 7×10^8 cpm/μg by random primer extension (16). Prehybridization for 24 h and hybridization for 24 h at 42°C in formamide solutions were carried out as previously described (61). After hybridization, membranes were washed five times in 2× SSC–0.3% sodium dodecyl sulfate for 5 min at room temperature and three times in 0.2× SSC–0.3% sodium dodecyl sulfate for 15 min at 55°C. Then membranes were placed between Kodak XAR-5 film and a Dupont Cronex intensifying screen at 70°C; the film was developed after 2 to 4 days. Relative mRNA levels were determined by scanning densitometry.

Potential transcriptional start sites were identified by primer extension with RNA isolated from vegetative DK1622 cells. The single-stranded oligonucleotide 5′dGGCGTCGGGGTCTCC3′, complementary to positions 1086 to 1100 in the *socA* sequence (39), was end labeled with [γ-^{32}P]ATP by using polynucleotide kinase. Labeled primer was purified with a Mermaid kit (BIO 101, Inc.) and added to 50 μg of total RNA in a volume of 10 μl containing 50 mM Tris HCl (pH 8.0) and 100 mM KCl. The mixture was heated to 95°C for 5 min with subsequent annealing at 65°C for 2 min and cooling at room temperature for 5 min. Extension was performed at 42°C for 90 min with avian myeloblastosis reverse transcriptase in a 30-μl volume containing 1 mM (each) dATP, dCTP, dGTP, and dTTP; 50 mM Tris-HCl (pH 8.3); 40 mM KCl; and 60 mM $MgCl_2$. One milliliter of 0.5 M EDTA was added to stop the reaction, and the reaction tube was subjected to RNase digestion at 37°C for 30 min. The reaction mixture was purified with a Mermaid kit, resuspended in Tris-EDTA buffer, and fractionated on an 8% polyacrylamide sequencing gel in parallel with dideoxynucleotide sequencing reactions primed with the same oligonucleotide (53).

Quantification of β-galactosidase activity. The specific activity of β-galactosidase was measured at intervals during development in nonspore and spore fractions by the method of Kroos and Kaiser (36), with modifications. Cells growing exponentially in CTT liquid were sedimented and resuspended in TPM buffer (10 mM Tris-HCl [pH 7.5], 1 mM $KH_2PO_4 \cdot K_2HPO_4$ [pH 7.6], 8 mM $MgSO_4$) at a density of 5×10^9 cells ml^{-1}. A 0.1-ml aliquot was added to 0.4 ml of TPM and stored at −20°C for later determination of β-galactosidase activity in growing cells (0-h sample). For development, 20-μl aliquots were spotted on TPM agar (TPM buffer plus 1.5% Difco agar) plates, incubated at 32°C, and scraped from the agar at various times into 0.5 ml of TPM buffer. Samples were stored at −20°C until all were collected; then they were thawed and placed on ice. All samples were sonicated twice with a standard microtip (W380; Heat Systems-Ultrasonics, Inc.) for 45 s each at 60 μW with ice-water cooling to disrupt rod-shaped cells. After the determination of the β-galactosidase specific activity of rod-shaped cells, sonication-resistant spores were washed with TPM buffer, sonicated for 3 min, and washed again with TPM buffer. Cell-free spore suspensions were disrupted in a minibead beater (Biospec Products) for 2 min with 75- to 150-μm-diameter acid-washed glass beads (Sigma) at 4°C. The specific activity of the spore sample was measured as previously described (36). Protein was assayed with bicinchoninic acid reagents (Pierce Chemical Co.) and bovine serum albumin standards. β-Galactosidase specific activity units are given in nanomoles of *o*-nitrophenol produced per minute per milligram of protein.

Extracellular complementation. Cells were grown in CTT broth to 5×10^8 ml^{-1}, harvested by centrifugation, and resuspended in TPM buffer at a density of 5×10^9 cells ml^{-1}. Strains were combined at ratios of 1:1, and 20-μl aliquots of cell mixtures were spotted on TPM agar and incubated at 32°C for 4 days. Plates were heated at 50°C for 2 h to kill rod-shaped cells. Fruiting bodies were resuspended in TPM buffer and sonicated to disperse spores (5 s at 60 μW cm^{-1}). Spores were counted by phase-contrast microscopy in a Petroff-Hausser chamber, diluted in TPM buffer, mixed with 3 ml of CTT soft agar, and plated on CTT agar to allow the spores to germinate. Plates were incubated at 32°C for 4 to 5 days, and colonies were transferred to CTT plates containing tetracycline (20 μg/ml).

RESULTS

Suppression restores C-signaling. There are two basic ways that *soc* mutations could cause the suppression of *csgA* defects. They could restore C-signal production via a CsgA-indepen-

TABLE 2. Extracellular complementation

Strain mixture	Viable spores	Complementation[a] (%)
DK1622 + LS523	4.9×10^6	49/299 (16)
LS559 + LS523	7.5×10^6	144/300 (48)
LS560 + LS523	4.9×10^6	100/300 (33)
LS523 + LS523	8	

[a] Number of spores derived from *csgA*/total number of spores tested.

dent pathway or activate a step in the C-signal response pathway in the absence of the C-signal. Only the former mechanism would result in the production of a signaling molecule that can be detected by extracellular complementation of *csgA* mutants. *csgA* (LS523) cells made tetracycline resistant were allowed to develop with tetracycline-sensitive *socC csgA* cells at a cell ratio of 1:1. The resulting myxospores were germinated under nonselective conditions and then transferred to plates containing tetracycline to determine the frequency of tetracycline-resistant *csgA* spores. *csgA* mutants temporarily regain the ability to develop when mixed with developing wild-type cells because of the acquisition of the C-signal from neighboring wild-type cells. The mixture of *csgA* cells with DK1622 (wild-type) cells increased the *csgA* spore number 10^5-fold; *csgA* spores were 16% of total spores (Table 2). The extracellular complementation of LS523 was even more efficient with LS559 (*socC559 csgA205*) or LS560 (*soc-560 csgA205*) in terms of total spore yield and the percentage of *csgA* cells stimulated to sporulate (Table 2). These results demonstrate that suppressor strains are able to employ an alternative, CsgA-independent method for the production of the C-signal or a C-signal-like effector.

SocC, a putative DNA-binding protein, regulates *socA* expression. The ΩLS559 transposon is inserted into *socC* (Fig. 1). The ΩLS560 transposon is located between the *socA* and *socB* genes and would also be expected to disrupt *socC* transcription since the 12-kb transposon separates *socB* and *socC* from the *socABC* regulatory region (39). While SocC does not have significant amino acid sequence identity with other sequences in the GenBank database (39), a putative helix-turn-helix (HTH) motif was detected near the N terminus by using the algorithm of Dodd and Egan (10). Using a reference set of 91 HTH sequences, Dodd and Egan assigned an SD score (standard deviation units relative to the appropriate mean) by weighting the probability of each amino acid appearing at a specific position within the HTH sequence. Authentic DNA-binding proteins have SD scores ranging from 2.5 to 6.0. The putative SocC HTH region, TSIQDLVDAMGVNKPSLYSI FG, achieved an SD score of 4.4, which indicates a >95% probability of this being a DNA binding domain (10). The most highly conserved residues in the SocC HTH motif are underlined and include a glycine in the turn and several hydrophobic residues which help the helices to pack against the rest of the protein (46).

The role of SocC in the regulation of *socABC* expression was examined with *soc-lacZ* fusions in *socC*$^+$ and *socC* mutant backgrounds. Tn*5 lac* contains a promoterless *lacZ* gene near one end of the transposon (35). In the orientation observed in the *socABC* operon, *lacZ* expression is under the control of the *socABC* regulatory region (Fig. 1). Translational stop codons within the transposon but upstream of *lacZ* ensure that transcriptional fusions are formed. The *socC559* allele contains a Tn*5 lac* insertion in *socC* which was cloned along with *socAB* and the entire upstream regulatory region (pLEE1) (39) and introduced into wild-type cells in which it integrated into the *socABC* operon by homologous recombination to generate a *socA*$^+$/*socA*$^+$ *socB*$^+$/*socB*$^+$ *socC-lacZ*/*socC*$^+$ merodiploid. Regulatory proteins usually work in *trans*, so this merodiploid is expected to express *lacZ* at levels reflective of the wild-type level of *socABC* expression. The *socC* mutant haploids, LS559 (*csgA205 socC559*) and LS620 (*socC559*), had 90-fold-higher levels of β-galactosidase specific activity during vegetative growth than those of the merodiploid LS293 (Table 3). (Note that the merodiploid also differs from the haploid derivative LS620 in that it has an altered *socA*/*socB*/*socC* gene ratio of 2:2:1 compared with 1:1:0 for the haploid. However, the major difference is the presence or absence of *socC*.) LS560, which is likely to be SocA$^+$ SocB$^-$ SocC$^-$ because of a transposon insertion between *socA* and *socB* (Fig. 1), showed a 40-fold increase in β-galactosidase specific activity compared with that of LS293. The presence of the *csgA* mutation in LS559 did not alter the level of expression from that observed with the otherwise isogenic *csgA*$^+$ derivative, LS620.

TABLE 3. SocC, a negative autoregulator of *socABC* operon transcription

Strain (genotype)	β-Galactosidase sp act[a]	Relative mRNA level[b]
DK1622 (wild type)	NA[c]	1
LS293 (*socC-lacZ*/*socC*$^+$)	50	2
LS620 (*socC559*)	4,500	98
LS559 (*socC559 csgA205*)	4,500	115
LS560 (*soc-560 csgA205*)	2,000	58

[a] Data are expressed in nanomoles of *o*-nitrophenol produced per minute per milligram of protein (37).
[b] Determined by scanning densitometry.
[c] NA, not applicable since DK1622 has no *socC-lacZ* fusion.

The possibility that *socA* is overexpressed in haploid mutant strains was further examined with an mRNA slot blot assay. The *socA* gene is upstream from both insertions and was used as a probe for *socA* transcription (Fig. 1). The *socA* mRNA level increased 50- to 100-fold in LS559 and about 30- to 60-fold in LS560 from those observed in the *socC*$^+$ merodiploid (LS293) and wild type (DK1622), respectively (Table 3). Therefore, both insertions lead to substantial overexpression of *socA* during vegetative growth.

Developmental *socA* expression was assessed by measuring β-galactosidase specific activity at intervals in cells and spores (Fig. 2). LS293, LS620, and LS559 cells showed decreased β-galactosidase specific activities over the course of development, while expression increased continuously in sporulating cells. The minor peak in β-galactosidase specific activity at 48 to 60 h may be due in part to artificial lysis of a portion of sporulating cells by sonication during the extraction of β-galactosidase; sporulating cells have not acquired full resistance to sonication at this developmental stage. By the end of development, the specific activity in spores is substantially higher than that in rod-shaped cells. The activity in LS295, which does not form fruiting bodies, remained relatively constant at the vegetative-cell levels. *socC*$^+$ strains (LS293 and LS295) have about 100-fold-lower levels of *lacZ* expression compared with those of *socC* mutant haploids (LS620 and LS559), although the pattern of expression remains quite similar (compare the results for LS293 and LS620 in Fig. 2). Apparently, the regulation of *socABC* operon expression is also influenced by as-yet-unknown factors which decrease expression in rod-shaped cells and increase expression in sporulating cells. Comparison of the *socA* expression assays (Fig. 2 [LS620 and LS559]) with similar assays using a *csgA-lacZ* transcriptional fusion (21, 41) revealed that *socA* expression in suppressor strains is at least 100-fold higher than *csgA* expression at all stages of development.

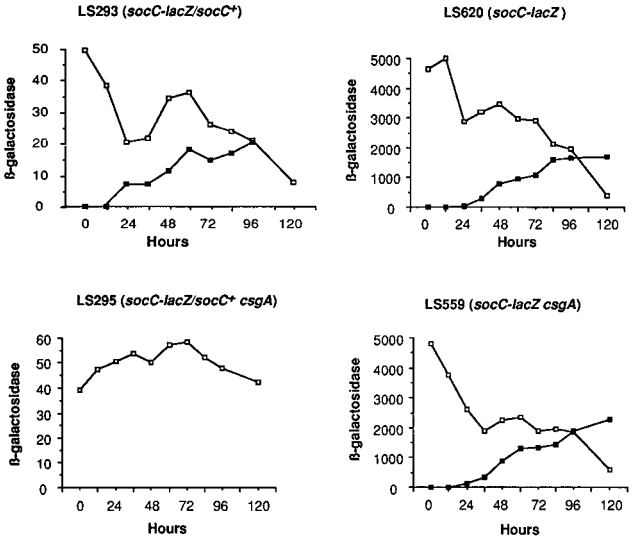

FIG. 2. Expression of a *socA-lacZ* transcriptional gene fusion during growth and development. β-Galactosidase specific activity was measured in extracts of rod-shaped cells (open squares) and spores (closed squares). β-Galactosidase specific activity at 0 h is activity in exponentially growing cells. Data are the averages of three independent experiments. LS295 is unable to develop.

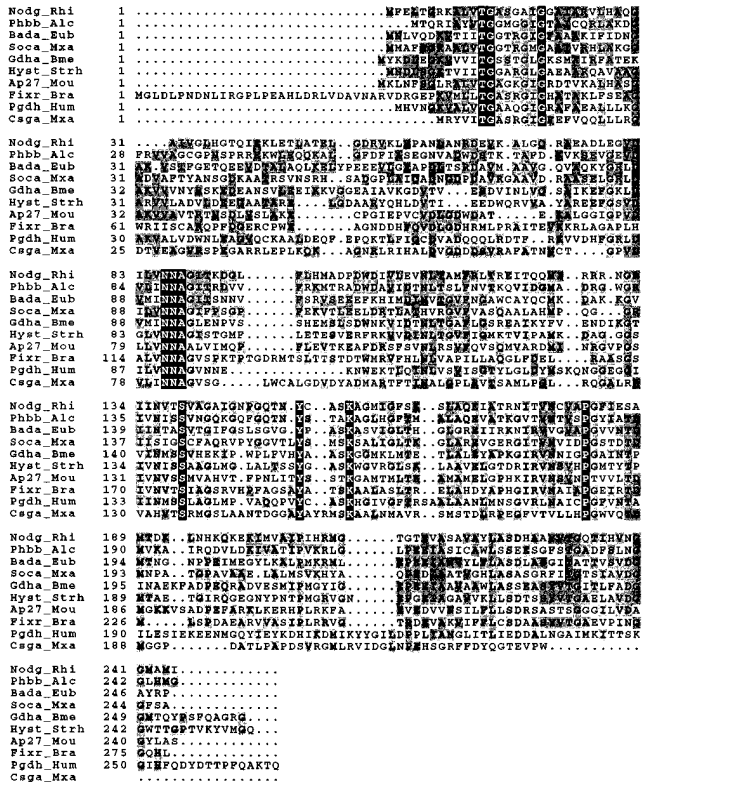

FIG. 3. Alignment of several SCAD gene products with CsgA and SocA. Nodg_Rhi, nodulation protein G from *Rhizobium meliloti* (6); Phbb_Alc, acetoacetyl-coenzyme A reductase from *Alcaligenes eutrophus* (48); Bada_Eub, 27K-2 protein from a *Eubacterium* sp. (17); Soca_Mxa, SocA from *M. xanthus* (39); Gdha_Bme, glucose dehydrogenase from *Bacillus megaterium* (43); Ap27_Mou, adipocyte p27 protein from the house mouse, *Mus musculus* (66); Hyst_Strh, 3α,20β-hydroxysteroid dehydrogenase from *Streptomyces hydrogenans* (44); Fixr_Bra, FixR protein from *Bradyrhizobium japonicum* (60); Pgdh_Hum, $NADP^+$-dependent prostaglandin dehydrogenase from humans (34); Csga_Mxa, CsgA protein from *M. xanthus* (21). There has been an addition of 63 amino acid residues to the CsgA N terminus proposed by Hagen and Shimkets (21) because of site-directed mutagenesis studies unambiguously defining the actual translational start codon (38). Black boxes with white letters indicate amino acids that are conserved in all sequences. Grey boxes with black letters indicate amino acids that predominate at a position.

SocA resembles CsgA. The overproduction of a protein with a function similar to that of CsgA could result in the production of the C-signal through an alternative pathway. At moderate stringency, *csgA* is the only gene that hybridizes with a *csgA* gene probe, indicating that *csgA* is unique at the nucleic acid sequence level (56). However, at the amino acid level, CsgA contains striking homology to SCADs (1, 39). SocA is also a member of this family and has 28% identity to CsgA (over the entire length of the protein) and 51% amino acid similarity. Alignment with several SCAD family members revealed that active-site amino acids conserved throughout the family (49) are also conserved in CsgA and SocA (Fig. 3). For example, the conserved TGG motif near the N terminus is part of a Rossmann fold that serves as the coenzyme binding site (18, 19) and is found in both CsgA and SocA (Fig. 3). The finding of a previous report that CsgA lacks this motif (1) was based on an incorrect proposed translation start site (21). The precise *csgA* translation start site has now been identified by site-directed mutagenesis and produces a 24.5-kDa protein with the TGG motif (38). The conserved threonine probably hydrogen bonds with coenzyme, stabilizing it in the coenzyme binding pocket in both 3α,20β-hydroxysteroid dehydrogenase (19) and CsgA (38). The conserved SYK motif near the center of the protein has been proposed to promote electrophilic attack on a carbonyl oxygen of the substrate, thereby allowing the transfer of a hydride ion from the reduced cofactor (18). A chemical modification of the conserved lysine inactivates 3α,20β-hydroxysteroid dehydrogenase (47). The replacement of the conserved tyrosine or lysine with other amino acids by site-directed mutagenesis inactivates *Drosophila* alcohol dehydrogenase (5). The replacement of the conserved serine and lysine with threonine and arginine, respectively, inactivated CsgA (38). The conservation of these amino acids in SocA and CsgA argues that both proteins are dehydrogenases.

Our working hypothesis for *csgA* suppression is that excessive SocA restores C-signaling. If this model is correct, *csgA* suppression should not occur in a *socA socC* strain. Attempts to create a *socA socC* disruption have been unsuccessful, suggesting that SocA has an essential function during vegetative growth (see Materials and Methods for descriptions of these experiments). The overexpression of SocA in a *socC*$^+$ background would also distinguish between these models; however, suitable *M. xanthus* expression vectors are not available.

SCAD family members catalyze reduction and oxidation reactions of a wide variety of simple and complex alcohols, many of which are signaling molecules in other organisms. Many of the most closely related SCAD members were grouped according to the type of substrate they utilize, and the amino acid identities and similarities of CsgA and SocA were calculated on the basis of pairwise comparisons with other members of the family. CsgA showed higher similarity (51%) and identity (28%) to SocA than it did to most other family members (Fig. 4). The closest relatives to SocA in the sequence databases are 3-oxoacyl reductases from plants and bacteria, which are involved in fatty acid biosynthesis and have 37 to 39% amino acid identity. CsgA also has highest homology with enzymes utilizing acyl substrates, for example, rat fatty acid synthase, human NADPH-dependent 15-hydroxyprostaglandin dehydrogenase, and human NADH-dependent 15-hydroxyprostaglandin dehy-

Enzyme	Accession #	Organism	CsgA S	CsgA I	SocA S	SocA I
A. Alcohol substrates						
Alcohol dehydrogenase	P07163	*Drosophila sp.*	45.4	21.6	44.9	25.3
	P25988	*Scaptomyza albovittata*	47.3	18.2	45.9	24.5
1,2-Dihydroxy-3,4-cyclohexadiene-1-carboxylate dehydrogenase	P23102	*Pseudomonas putida*	44.3	21.5	55.8	31.8
	P07772	*Acinetobacter calcoaceticus*	41.5	21.0	54.0	29.5
2,3-Dihydro-2,3-dihydroxy-benzoate dehydrogenase	P15047	*Escherichia coli*	50.7	27.0	56.7	35.6
Biphenyl dihydrodiol dehydrogenase	P08694	*Pseudomonas pseudoalcaligenes*	49.0	25.9	58.2	30.5
cis-1,2-dihydrobenzene-1,2-diol dehydrogenase	P08088	*Pseudomonas putida*	50.0	27.9	55.8	33.3
B. Carbohydrate substrates						
Glucose dehydrogenase	P07999	*Bacillus megaterium*	44.1	19.8	53.5	25.7
	P10528	*Bacillus megaterium*	40.9	20.3	54.3	26.9
	P12310	*Bacillus subtilis*	43.0	19.0	54.9	27.5
Ribitol dehydrogenase	P00335	*Klebsiella aerogenes*	39.6	22.5	45.6	25.9
Sorbitol-6-phosphate dehydrogenase	P05707	*Escherichia coli*	47.1	21.5	47.5	26.7
N-acylmannosamine 1-dehydrogenase	P22441	*Flavobacterium sp.*	49.1	26.0	57.7	33.5
C. Acyl substrates (Fatty acids/Polyketides/Poly-ß-hydroxybutyrate)						
3-oxoacyl-[acyl carrier protein] reductase	P25716	*Escherichia coli*	51.6	26.5	56.8	37.8
	P28643	*Cuphea lanceolata*	47.1	24.4	55.9	34.3
	P27582	*Brassica napus*	48.4	24.2	61.4	39.3
	P12785	*Rattus norvegicus*	55.3	28.8	45.3	20.4
Acetoacetyl-CoA reductase	P14697	*Alcaligenes eutrophus*	46.6	26.0	55.0	31.8
	P23238	*Zoogloea ramigera*	51.6	22.4	55.0	34.7
Keto-acyl reductase	P16542	*Streptomyces violaceoruber*	46.6	22.0	54.3	33.7
	P16543	*Streptomyces violaceoruber*	48.8	26.5	50.8	30.4
	P16544	*Streptomyces coelicolor*	46.6	27.4	55.3	31.8
NADH-dependent 15-hydroxy-prostaglandin dehydrogenase	P15428	*Homo sapiens*	49.5	28.1	51.9	27.8
NADPH-dependent 15-hydroxy-prostaglandin dehydrogenase	P16152	*Homo sapiens*	52.7	28.6	48.2	28.5
D. Steroid substrates						
7-alpha-hydroxysteroid dehydrogenase	P25529	*Escherichia coli*	45.5	25.0	48.9	28.9
3-α,20-ß-hydroxysteroid dehydrogenase	P19992	*Streptomyces hydrogenans*	49.8	27.0	55.6	32.4
3-ß-hydroxysteroid dehydrogenase	P19871	*Comomonas testosteroni*	49.8	21.4	53.9	33.6
Bile acid 7-dehydroxylase	P19337	*Eubacterium sp.*	49.1	23.0	53.7	33.1
	P07914	*Eubacterium sp.*	49.1	24.3	53.7	33.1
Corticosteroid 11-ß-dehydrogenase	P16232	*Rattus norvegicus*	48.0	22.8	42.7	24.4
Estradiol 17-ß-dehydrogenase	P14061	*Homo sapiens*	50.2	26.9	53.0	30.1
E. Unknown substrates						
Adipocyte 27	P08074	*Mus musculus*	49.5	25.7	56.4	34.3
C-signal protein CsgA	L27429	*Myxococcus xanthus*	self		51.0	28.2
Suppressor of C signal SocA	L27430	*Myxococcus xanthus*	51.0	28.2	self	
DoxE	S27635	*Pseudomonas sp.*	48.4	29.3	52.9	27.7
Nodulation protein NodG	P17611	*Azospirillum brasilense*	47.7	23.6	54.7	31.7
Nitrogen fixation FixR	P05406	*Bradyrhizobium japonicum*	50.5	31.4	52.3	26.6

FIG. 4. Comparisons of the amino acid similarities and identities of CsgA and SocA to other SCAD family members, grouped according to substrate utilization. Alignment was carried out by using the computer program GAP (9) with a gap weight of 3.00 and a length weight of 0.10. Data are percentages of amino acid similarity (S) and identity (I) from pairwise alignments over the entire lengths of the two proteins. The most closely related sequences are underlined.

drogenase. However, CsgA was less closely related to family members of known function than was SocA.

The *socABC* regulatory region. During development, *socA* expression decreased in cells and increased in spores. This cell-type-specific regulation of expression prompted a closer examination of the *socA* regulatory region. Two apparent transcriptional start sites were identified by primer extension of mRNA isolated from vegetative cells (Fig. 5). These two putative promoter sequences were compared with other *M. xanthus* promoter sequences (Fig. 6). The upstream start site (P1) had promoter sequences at −35 and −10 similar to those of the *M. xanthus vegA* promoter (33), and the downstream start site (P2) had promoter sequences similar to those of the *E. coli* σ^{70} consensus (23). Since little is known about *M. xanthus* promoters, 20 bp in the −10 regions of the putative P1 and P2 promoters were deleted, and the constructs were integrated into the chromosome at the phage Mx8 attachment site *attB* (Fig. 7A). The β-galactosidase specific activities of these strains were compared with that of LS641, which contains intact *socA* promoter sequences integrated at the same site. LS641 showed about half the β-galactosidase specific activity of LS293, which contains the same plasmid integrated into the *socABC* operon (Fig. 7B). When promoter sequences are moved into *attB*, promoter activities are reduced by 50% for unknown reasons (40). Deletion of the −10 region of P2 (ΔP2) decreased *socABC* operon expression by approximately two-thirds in vegetative cells and 84-h developing cells, suggesting that P2 is a promoter. In the primer extension assay, the stronger signal intensity derived from P2 is consistent with this result (Fig. 5). Deletion of the −10 region of P1 (ΔP1) did not reduce *socA* expression in either vegetative cells or 84-h developing cells; it remains possible that the −10 region of P1 is not an essential region of the promoter (Fig. 7). The proposed −10 region from the *vegA* promoter has not been shown to be essential for *vegA* expression (33).

DISCUSSION

The finding that *csgA* mutants containing transposon insertions in the *socABC* operon regain the ability to develop pre-

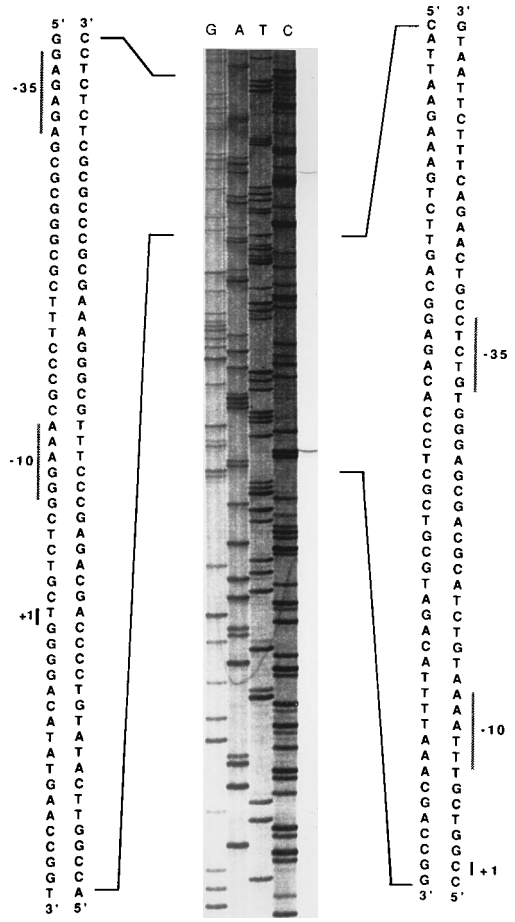

FIG. 5. The putative *socABC* operon transcriptional start sites determined by primer extension of RNA from vegetative cells. An oligonucleotide complementary to *socA* mRNA was used for both reverse transcriptase primer extension (far right lane) and nucleotide sequencing. The DNA sequences of the putative promoter regions are shown to the left and right of the gel. +1, putative transcriptional start site, with P1 on the left and P2 on the right. The −35 and −10 regions are indicated by gray lines.

	-35		-10	
E. coli σ^{70} consensus	TTGACA	17	TATAAT	
vegA	TAGACA	18	AAGGGT	Vegetative
socA P1	GAGAGA	18	AAAGGG	Vegetative
socA P2	GAGACA	18	TTTAAA	Vegetative
ops	TTGCAT	18	AATGCT	Developmental
tps	TTGCTC	17	CAAGCT	Developmental
csgA	TTGCCA	18	GTTAAT	Developmental
E. coli σ 54	CTGGCACGGCCTTTGCA			
mbhA	ATGGCACGCCATCTGCT			Developmental

FIG. 6. Alignment of the DNA sequences of *M. xanthus* promoters *vegA* (33), *tps* and *ops* (25), *mbhA* (51), *csgA* (41), *socA* P1 and *socA* P2 (this study), *E. coli* σ^{54} (45), and *E. coli* σ^{70} consensus (23).

sents a conundrum. How can a null mutation in the *socC* coding sequence restore development to a strain with a null mutation in the *csgA* gene? Suppressor mutations appear to produce a C-signal-like molecule by a CsgA-independent pathway since strains containing suppressor mutations extracellularly complement *csgA* mutants. The model that has emerged from this work is that the inactivation of SocC, a putative DNA-binding protein, results in the overproduction of SocA, which restores C-signaling. SocA and CsgA have 28% amino acid identity and 51% similarity. Attempts to directly demonstrate that SocA overproduction is responsible for *csgA* suppression are complicated by an inability to generate a *socA* null allele; apparently, *socA* is an essential gene.

The nature of the C-signal is currently unknown. Although it has been proposed that CsgA is the C-signal (29), work presented here and elsewhere (38) raises the possibility that CsgA is an enzyme which manufactures the C-signal. The suppression model predicts that SocA and CsgA are enzymes with overlapping substrate specificities. There are three pieces of evidence in support of this notion. First, the open configuration of the active site in a SCAD member enables the binding and catalysis of structurally different substrates. For example, NADP-dependent 15-hydroxyprostaglandin dehydrogenase initiates the process of prostaglandin degradation by converting the 15-hydroxy form to the 15-keto form. The same enzyme also acts on the 9-keto group in the reverse direction to convert prostaglandin E_2 to prostaglandin $F_{2\alpha}$ (3, 4, 22). Quinones are even better substrates (26, 67). This has led to the assignment of three different EC numbers to this enzyme (EC 1.1.1.141, EC 1.1.1.184, and EC 1.1.1.189). In view of the remarkable range of substrates utilized by individual family members, it is not unreasonable to hypothesize that SocA and CsgA have overlapping substrate specificities. At the same time, this observation suggests that identifying the biologically relevant substrates for SocA and CsgA may prove to be challenging. The second piece of evidence was derived by site-directed mutagenesis of conserved amino acids in CsgA and suggests that both

A.

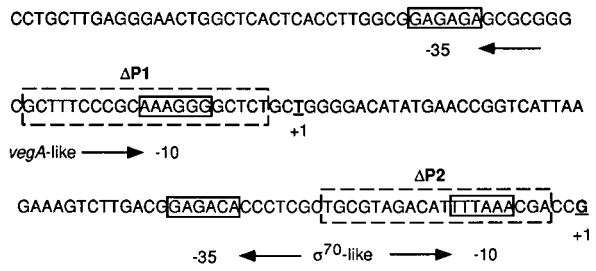

B.

	ß-galactosidase	
	Veg	84 hr
LS641 (*socA-lacZ*)	25.0 ± 3	15.0 ± 2
LS642 (ΔP1 *socA-lacZ*)	24.0 ± 4	20.0 ± 3
LS643 (ΔP2 *socA-lacZ*)	9.7 ± 2	10.0 ± 1

FIG. 7. Locations of the two *socABC* operon promoter deletion mutations and the effects of these deletions on *socA-lacZ* expression. (A) The −35 and −10 regions are enclosed in small boxes. The deletion mutations are outlined with large dotted boxes. Arrows show the spacing between the −35 and −10 regions. Two putative transcriptional start sites (+1) are in bold type and underlined. (B) *socABC* operon expression measured in vegetative cells (Veg) and 84-h developing cells (84 hr). LS641 contains the wild-type regulatory region preceding the *socA-lacZ* fusion and is inserted into the chromosomal *attB* site. The strains containing promoter deletion mutations were constructed by inserting plasmid pLEE43 (ΔP1) and pLEE44 (ΔP2) into the *attB* site of DK1622 (wild type) to generate LS642 and LS643, respectively.

the coenzyme binding pocket and catalytic site are essential for C-signaling. Amino acid substitutions in the CsgA coenzyme binding site and catalytic pocket produce proteins that are unable to mediate C-signaling (38). This was particularly obvious with CsgA T-6→A, which was unable to bind coenzyme in vitro or to stimulate development when added to *csgA* cells submerged under a layer of buffer. The notion that CsgA is an enzyme is also indirectly supported by the fact that it is much larger than peptide hormones found in other bacterial systems. Finally, there is evidence that NAD(P) is preferred over NAD(P)H during C-signaling. When CsgA is added to *csgA* cells submerged under a layer of buffer, 10 μM NAD(P) stimulates development and 10 μM NAD(P)H delays development (38). These three pieces of evidence provide tantalizing clues that CsgA and SocA may participate in C-signaling through an enzymatic mechanism.

Members of the SCAD family are involved in the reduction and oxidation of a wide variety of compounds, making it difficult to deduce what the substrates for CsgA and SocA might be. SocA exhibited highest homology with SCAD members involved in fatty acid biosynthesis. The most obvious potential substrates or products on the *Myxococcus* surface include the many types of 2- and 3-hydroxy fatty acids in membrane lipids (15, 68) and 3-hydroxy fatty acids in lipopolysaccharide (52). While there is a substantial carbohydrate component to the cell surface, including exopolysaccharides, fibrils, lipopolysaccharide, and peptidoglycan, the homologies with carbohydrate-utilizing SCAD enzymes were lower than those with enzymes with acyl substrates. Fatty acids are intercellular signals in sponges in which cells aggregate in response to arachidonic acid and docosahexaenoic acid (65). Prostaglandins and related molecules are involved in plant and animal cell-cell communications (14, 34, 59). NodRm IV-S, one of the nodulation factors involved in legume-*Rhizobium* communication, is an acylated β-1,4-tetrasaccharide, and a chemical modification of the fatty acid chains eliminated biological activity (64). The *Myxococcus* E-signal, which seems to be upstream of the C-signal in the developmental program, may consist of one or more branched-chain fatty acids (12, 63). It would not be terribly surprising if a fatty acid emerged as the C-signal since the hydrophobic nature of a fatty acid would enable it to be sequestered at the cell surface. The C-signal is not diffusible (29), and it is likely that C-signaling is a tactile response to contact between cell surfaces (30, 31).

CsgA clearly participates in a novel type of tactile signaling system, and CsgA is the first member of the SCAD family that is cell surface associated. The extent to which this type of signaling system occurs in other organisms remains unknown. Members of the SCAD family are required for heterocyst formation in *Anabaena* spp. (2), for mouse adipocyte differentiation (66), and for sex determination in maize (7), though the roles of the SCAD genes in these cases have not yet been elucidated.

ACKNOWLEDGMENTS

We thank Colin Hughes for critically reading the manuscript.
This work was supported by NSF grant MCB9304083.

REFERENCES

1. **Baker, M.** 1994. *Myxococcus xanthus* C-factor, a morphogenic paracrine signal, is similar to *E. coli* 3-ketoacyl-acyl carrier protein reductase and human 17β-hydroxysteroid dehydrogenase. Biochem. J. **301:**311–312.
2. **Black, T. A., and C. P. Wolk.** 1994. Analysis of a Het$^-$ mutation in *Anabaena* sp. strain PCC 7120 implicates a secondary metabolite in the regulation of heterocyst spacing. J. Bacteriol. **176:**2282–2292.
3. **Chang, D. G. B., M. Sun, and H. H. Tai.** 1981. Prostaglandin 9-ketoreductase/type II 15-hydroxyprostaglandin dehydrogenase is not a prostaglandin specific enzyme. Biochem. Biophys. Res. Commun. **101:**898–904.
4. **Chang, D. G. B., and H. H. Tai.** 1981. Prostaglandin 9-ketoreductase and type II 15-hydroxyprostaglandin dehydrogenase from swine kidney are alternate activities of a single enzyme protein. Biochem. Biophys. Res. Commun. **99:**745–741.
5. **Chen, Z., J. C. Jiang, Z.-G. Lin, W. R. Lee, M. E. Baker, and S. H. Chang.** 1993. Site-specific mutagenesis of *Drosophila* alcohol dehydrogenase: evidence for involvement of tyrosine-152 and lysine-156 in catalysis. Biochemistry **32:**3342–3346.
6. **Debelle, F., and S. B. Sharma.** 1986. Nucleotide sequence of *Rhizobium meliloti* RCR2011 genes involved in host specificity of nodulation. Nucleic Acids Res. **14:**7453–7472.
7. **Delong, A., A. Calderon-Urrea, and S. L. Dellaporta.** 1993. Sex determination gene TASSELSEED2 of maize encodes a short chain alcohol dehydrogenase required for stage-specific floral organ abortion. Cell **74:**757–768.
8. **Deng, W. P., and J. A. Nickoloff.** 1992. Site-directed mutagenesis of virtually any plasmid by eliminating a unique site. Anal. Biochem. **200:**81–88.
9. **Devereux, J., P. Haeberli, and O. Smithies.** 1984. A comprehensive set of sequence analysis programs for the VAX. Nucleic Acids Res. **12:**387–395.
10. **Dodd, I. B., and J. B. Egan.** 1990. Improved detection of helix-turn-helix DNA-binding motifs in protein sequences. Nucleic Acids Res. **18:**5019–5026.
11. **Downard, J., S. V. Ramaswamy, and K.-S. Kil.** 1993. Identification of *esg*, a genetic locus involved in cell-cell signaling during *Myxococcus xanthus* development. J. Bacteriol. **175:**7762–7770.
12. **Downard, J., and D. Toal.** 1995. Branched chain fatty acids: the case for a novel form of cell-cell signaling during *Myxococcus xanthus* development. Mol. Microbiol. **16:**171–175.
13. **Dworkin, M., and D. Kaiser (ed.).** 1993. Myxobacteria II. American Society for Microbiology, Washington, D.C.
14. **Farmer, E. E., and C. A. Ryan.** 1990. Interplant communication: airborne methyl jasmonate induces synthesis of proteinase inhibitors in plant leaves. Proc. Natl. Acad. Sci. USA **87:**7713–7716.
15. **Fautz, E., G. Rosenfelder, and L. Grotjahn.** 1979. Iso-branched 2- and 3-hydroxy fatty acids as characteristic lipid constituents of some gliding bacteria. J. Bacteriol. **140:**852–858.
16. **Feinberg, A. P., and B. Vogelstein.** 1983. A technique for radiolabeling DNA restriction endonuclease fragments to high specific activity. Anal. Biochem. **132:**6–13.
17. **Franklund, C. V., P. D. Prada, and P. B. Hylemon.** 1990. Purification and characterization of a microbial, NADP-dependent bile acid alpha-hydroxysteroid dehydrogenase. J. Biol. Chem. **265:**9842–9849.
18. **Ghosh, D., Z. Wawrzak, C. M. Weeks, W. L. Duax, and M. Erman.** 1994. The refined three-dimensional structure of 3a, 20β-hydroxysteroid dehydrogenase and possible roles of the residues conserved in short-chain dehydrogenases. Structure (London) **2:**629–640.
19. **Ghosh, D., C. M. Weeks, P. Grochulski, W. L. Duax, M. Erman, R. L. Rimsay, and J. C. Orr.** 1991. Three-dimensional structure of holo 3α,20β-hydroxysteroid dehydrogenase: a member of a short-chain dehydrogenase family. Proc. Natl. Acad. Sci. USA **88:**10064–10068.
20. **Hagen, D. C., A. P. Bretscher, and D. Kaiser.** 1978. Synergism between morphogenetic mutants of *Myxococcus xanthus*. Dev. Biol. **64:**284–296.
21. **Hagen, T. J., and L. J. Shimkets.** 1990. Nucleotide sequence and transcriptional products of the *csg* locus of *Myxococcus xanthus*. J. Bacteriol. **172:**15–23.
22. **Hassid, A., and L. Levine.** 1977. Multiple molecular forms of prostaglandin 15-hydroxydehydrogenase and 9-ketoreductase in chicken kidney. Prostaglandins **13:**503–516.
23. **Helmann, J. D., and J. J. Chamberlin.** 1988. Structure and function of bacterial sigma factors. Annu. Rev. Biochem. **57:**839–872.
24. **Hodgkin, J., and D. Kaiser.** 1977. Cell-to-cell stimulation of movement in nonmotile mutants of *Myxococcus*. Proc. Natl. Acad. Sci. USA **74:**2938–2942.
25. **Inouye, S.** 1984. Identification of a developmentally-specific promoter of *Myxococcus xanthus*. J. Mol. Biol. **174:**113–120.
26. **Jarabak, J., A. Luncsford, and D. Berkowitz.** 1983. Substrate specificity of three prostaglandin dehydrogenases. Prostaglandins **26:**849–868.
27. **Johnson, R. C., and W. S. Reznikoff.** 1981. Localization of the Tn*5* transposase promoter using the cycling reaction of RNA polymerase. Nucleic Acids Res. **9:**1873–1883.
28. **Kim, S. K., and D. Kaiser.** 1990. Purification and properties of *Myxococcus xanthus* C-factor, an intercellular signaling protein. Proc. Natl. Acad. Sci. USA **87:**3635–3639.
29. **Kim, S. K., and D. Kaiser.** 1990. C-factor: a cell-cell signaling protein required for fruiting body morphogenesis of *M. xanthus*. Cell **61:**19–26.
30. **Kim, S. K., and D. Kaiser.** 1990. Cell motility is required for the transmission of C-factor, an intercellular signal that coordinates fruiting body morphogenesis of *Myxococcus xanthus*. Genes Dev. **4:**896–905.
31. **Kim, S. K., and D. Kaiser.** 1990. Cell alignment is required in differentiation of *M. xanthus*. Science **249:**926–928.
32. **Kim, S. K., and D. Kaiser.** 1991. C-factor has distinct aggregation and sporulation thresholds during *Myxococcus* development. J. Bacteriol. **173:**1722–1728.
33. **Komano, T., T. Franceschini, and S. Inouye.** 1987. Identification of a vege-

tative promoter in *Myxococcus xanthus*: a protein that has homology to histones. J. Mol. Biol. **196:**517–524.
34. **Krook, M., D. Ghosh, R. Stromberg, M. Carlquist, and H. Jornvall.** 1993. Carboxyethyllysine in a protein: native carbonyl reductase/NADP+-dependent prostaglandin dehydrogenase. Proc. Natl. Acad. Sci. USA **90:**502–506.
35. **Kroos, L., and D. Kaiser.** 1984. Construction of Tn*5 lac*, a transposon that fuses *lacZ* expression to exogenous promoters, and its introduction into *Myxococcus xanthus*. Proc. Natl. Acad. Sci. USA **81:**5816–5820.
36. **Kroos, L., and D. Kaiser.** 1987. Expression of many developmentally regulated genes in *Myxococcus* depends on a sequence of cell-cell interactions. Genes Dev. **1:**840–854.
37. **Kroos, L., A. Kuspa, and D. Kaiser.** 1986. A global analysis of developmentally regulated genes in *Myxococcus xanthus*. Dev. Biol. **117:**252–266.
38. **Lee, B.-U., K. Lee, J. Robles, and L. J. Shimkets.** 1995. A tactile sensory system of *Myxococcus xanthus* involves an extracellular NAD(P)+-containing protein. Genes Dev. **9:**2964–2973.
39. **Lee, K., and L. J. Shimkets.** 1994. Cloning and characterization of the *socA* locus which restores development to *Myxococcus xanthus* C-signaling mutants. J. Bacteriol. **176:**2200–2209.
40. **Li, S., and L. J. Shimkets.** 1988. Site-specific integration and expression of a developmental promoter in *Myxococcus xanthus*. J. Bacteriol. **170:**5552–5556.
41. **Li, S., B. Lee, and L. J. Shimkets.** 1992. *csgA* expression entrains *Myxococcus xanthus* development. Genes Dev. **6:**401–410.
42. **Li, S.-F., and L. J. Shimkets.** 1993. Effect of *dsp* mutations on the cell-to-cell transmission of CsgA in *Myxococcus xanthus*. J. Bacteriol. **175:**3648–3652.
43. **Makino, Y., S. Negoro, I. Urabe, and H. Okada.** 1989. Stability-increasing mutants of glucose dehydrogenase from *Bacillus megaterium* IWG3. J. Biol. Chem. **264:**6381–6385.
44. **Marekov, L., M. Krook, and H. Jornvall.** 1990. Prokaryotic 20-hydroxysteroid dehydrogenase is an enzyme of the 'short chain, non-metalloenzyme' alcohol dehydrogenase type. FEBS Lett. **266:**51–54.
45. **Morett, E., and M. Buck.** 1989. *In vivo* studies of the interaction of RNA polymerase-σ^{54} with the *Klebsiella pneumoniae* and *Rhizobium meliloti nifH* promoters: the role of NifA in the formation of an open promoter complex. J. Mol. Biol. **210:**65–77.
46. **Pabo, C. O., and R. T. Sauer.** 1992. Transcription factors: structural families and principles of DNA recognition. Annu. Rev. Biochem. **61:**1053–1095.
47. **Pasta, P., G. Mazzola, and G. Carrea.** 1987. Chemical modification of 3α, 20β-hydroxysteroid dehydrogenase. Biochemistry **26:**1247–1251.
48. **Peoples, O. P., and A. J. Sinskey.** 1989. Poly beta-hydroxybutyrate biosynthesis in *Alcaligenes eutrophus* H16. Characterization of the genes encoding beta-ketothiolase and acetoacetyl-CoA reductase. J. Biol. Chem. **264:**15293–15297.
49. **Persson, B., M. Krook, and H. Jornvall.** 1991. Characteristics of short-chain alcohol dehydrogenases and related enzymes. Eur. J. Biochem. **200:**537–543.
50. **Rhie, H. G., and L. J. Shimkets.** 1989. Developmental bypass suppression of *Myxococcus xanthus csgA* mutations. J. Bacteriol. **171:**3268–3276.
51. **Romeo, J. M., and D. R. Zusman.** 1991. Transcription of the myxobacterial hemagglutinin gene is mediated by a σ^{54}-like promoter and a *cis*-acting upstream regulatory region of DNA. J. Bacteriol. **173:**2969–2976.
52. **Rosenfelder, G., O. Luderitz, and O. Westphal.** 1974. Composition of lipopolysaccharides from *Myxococcus fulvus* and other fruiting and non-fruiting myxobacteria. Eur. J. Biochem. **44:**411–420.
53. **Sanger, F., S. Nicklen, and A. R. Coulson.** 1977. DNA sequencing with chain-terminating inhibitors. Proc. Natl. Acad. Sci. USA **74:**5463–5467.
54. **Shimkets, L. J.** 1990. Social and developmental biology of the myxobacteria. Microbiol. Rev. **54:**473–501.
55. **Shimkets, L. J., and S. J. Asher.** 1988. Use of recombination techniques to examine the structure of the *csg* locus of *Myxococcus xanthus*. Mol. Gen. Genet. **211:**63–71.
56. **Shimkets, L. J., R. E. Gill, and D. Kaiser.** 1983. Developmental cell interactions in *Myxococcus xanthus* and *spoC* locus. Proc. Natl. Acad. Sci. USA **80:**1406–1410.
57. **Shimkets, L. J., and D. Kaiser.** 1982. Induction of coordinated movement of *Myxococcus xanthus* cells. J. Bacteriol. **152:**451–461.
58. **Shimkets, L. J., and H. Rafiee.** 1990. CsgA, an extracellular protein essential for *Myxococcus xanthus* development. J. Bacteriol. **172:**5299–5306.
59. **Song, W. C., and A. R. Brash.** 1991. Purification of an allene oxide synthase and identification of the enzyme as cytochrome P-450. Science **253:**781–784.
60. **Thoeny, B., H. M. Fischer, D. Anthamatten, T. Bruderer, and H. Hennecke.** 1987. The symbiotic nitrogen fixation regulatory operon (*fixR nifA*) of *Bradyrhizobium japonicum* is expressed aerobically and is subject to a novel, *nifA*-independent type of activation. Nucleic Acids Res. **15:**8479–8499.
61. **Thomas, P. S.** 1980. Hybridization of denatured RNA and small DNA fragments transferred to nitrocellulose. Proc. Natl. Acad. Sci. USA **77:**5201–5205.
62. **Thomas, P. S.** 1983. Hybridization of denatured RNA transferred or dotted to nitrocellulose. Methods Enzymol. **100:**255–266.
63. **Toal, D., S. W. Clifton, B. A. Roe, and J. Downard.** 1995. The *esg* locus of *Myxococcus xanthus* encodes the E1α and E1β subunits of a branched-chain keto acid dehydrogenase. Mol. Microbiol. **16:**177–189.
64. **Truchet, G., P. Roche, and P. Lerouge.** 1991. Sulphated lipooligosaccharide signals of *Rhizobium meliloti* elicit root nodule organogenesis in alfalfa. Nature (London) **351:**670–673.
65. **Weissmann, G., W. Riesen, S. Davidson, and W. Moseley.** 1988. Stimulus-response coupling in marine sponge cell aggregation: lipid metabolism and the function of exogenously added arachidonic and docosahexaenoic acids. Biochim. Biophys. Acta **960:**351–364.
66. **Wenz, H. M., L. Hinck, P. Cannon, M. Navre, and G. Ringold.** 1992. Reduced expression of AP27 protein, the product of a growth factor-repressible gene, is associated with diminished adipocyte differentiation. Proc. Natl. Acad. Sci. USA **89:**1065–1069.
67. **Wermuth, B.** 1981. Purification and properties of an NADPH-dependent carbonyl reductase from human brain. J. Biol. Chem. **256:**1206–1213.
68. **Yamanaka, S., R. Fudo, A. Kawaguchi, and K. Komagata.** 1988. Taxonomic significance of hydroxy fatty acids in myxobacteria with special reference to 2-hydroxy fatty acids in phospholipids. J. Gen. Appl. Microbiol. **34:**57–66.